Chemical Engineering & Processing: Process Intensification 191 (2023) 109467

Contents lists available at ScienceDirect

Chemical Engineering and Processing - Process Intensification

journal homepage: www.elsevier.com/locate/cep

Topological flow transformations in a universal vortex bioreactor

Igor V. Naumov [a,b,*], Ruslan G. Gevorgiz [a,c], Sergey G. Skripkin [a,b], Maria V. Tintulova [a,b], Mikhail A. Tsoy [a], Bulat R. Sharifullin [a]

[a] Kutateladze Institute of Thermophysics SB RAS, 1, Lavrentyev Ave., Novosibirsk, 630090, Russian Federation
[b] Novosibirsk State University, 1, Pirogova Str., Novosibirsk, 630090, Russian Federation
[c] Kovalevsky Institute of Biology of the Southern Seas of RAS, 38, Leninsky Ave., Moscow, 119991, Russian Federation

ARTICLE INFO

Keywords:
Vortex flows
Marine microalgae
Aerial bioreactor, complex vortex
Vortex flow modeling

ABSTRACT

Research into the flow structure in an aerial vortex bioreactor is relevant for developing the methods to grow cell cultures. It is especially important in the case when, with the culture growth in the bioreactor, such parameters of the medium as density and viscosity can significantly change, accordingly altering the characteristic flow regimes. Since the cultivated culture is not transparent in most cases, it is impossible to visually determine the flow regime. Therefore, a detailed study of the regularities of flow regimes in an aerial vortex reactor is of great fundamental and applied interest. The research was carried out in an 8.5 L universal glass aerial vortex bioreactor, with a washer freely floating on its surface and stabilizing the motion of the working fluid. The regularities of the vortex motion of the culture medium depend on its volume and the rotation intensity of the activator generating vortex motion in the air. The air vortex generated by the impeller (activator) above the liquid surface spins the working fluid and a free-floating washer. The study reveals that despite the complex configuration of the flow stabilizing device (a free-floating washer), the observed vortex structure and its dynamics with increasing flow swirl intensity coincides with the structure of a confined vortex flow in a cylindrical container for both single-fluid and immiscible two-fluid configurations.

1. Introduction

The development and construction of bioreactors is crucial in modern biotechnology for the intensive cultivation of cells, tissues, and microorganisms. There are various specialized and universal bioreactor designs that have been created to ensure optimal cultivation conditions [1–5] The productivity of cell cultures and tissues is improved by paying special attention to the efficiency of mass transfer and increasing the biosynthesis rates of target metabolites. Techniques for providing immobilized cells with nutrients and various methods for mixing suspension cultures have been developed, leading to the creation of novel bioreactor structures such as airlift, membrane, film, and column types [6–9]. Bioreactors with mechanical [10,11] and pneumatic stirring [12] are the most commonly used in biotechnological practice for deep cultivation of cells, tissues, and microorganisms [13]. This is due to their simplicity and cost-effectiveness for both laboratory and industrial-scale cultivation, rather than their optimal fluid motion. Various studies have attempted to optimize mixing cell suspensions using different mixing and bubbling devices [11]. However, due to the challenges of physically analyzing processes and phenomena in a bioreactor with an actively growing culture, as well as the lack of reliable measuring equipment, these attempts have been mostly empirical, and scaling up research results has been difficult [14].

Although mechanical and bubbling mixing are commonly used in bioreactors for cell and tissue cultivation, they have limitations. Mechanical stirring can cause cell injury due to hydraulic shock, temperature changes, and shear stresses, especially with viscous nutrient media [15]. Bubbling mixing can result in poor mixing of viscous media, excessive foaming, and cell death from bubbles collapsing on the surface [16,17]. Both methods can also create hydrodynamic shadows and areas of increased turbulence, which make it challenging to cultivate microorganisms with high density [18] or cells and tissues with low membrane strength [19,20]. To address these limitations, bioreactor designs that use free rotation or vertical swinging have been developed [1,4,21,22]. However, these designs have limited volume and scalability.

A breakthrough in bioreactor development was achieved through the use of vortex mixing, which mimics natural phenomena such as tornadoes. Researchers have developed several bioreactor designs with a new type of vortex mixing and have demonstrated its effectiveness

* Corresponding author.
E-mail address: naumov@itp.nsc.ru (I.V. Naumov).

https://doi.org/10.1016/j.cep.2023.109467
Received 29 March 2023; Received in revised form 23 May 2023; Accepted 18 June 2023
Available online 20 June 2023

Nomenclature

H	height of the bioreactor vessel (mm)
h	height of the working fluid (mm)
h_{fw}	height of the washer (mm)
K_La	oxygen mass transfer rate
PIV	Particle image velocimetry
R	radius of the bioreactor vessel (mm)
R_{fw}	radius of the washer (mm)
r_{wi}	washer bore radius (mm)
Re	Reynolds number
V_{ang}	linear velocity of the washer rotation (mm/s)
V_{ax}	axial velocity component (mm/s)
V_r	radial velocity components (mm/s)
V_{tg}	azimuthal velocity components (mm/s)
ρ_w	density of distilled water (kg/m^3)
ρ_g	density of water–glycerol solution (kg/m^3)
ν_w	kinematic viscosity of distilled water (mm^2/s)
ν_g	kinematic viscosity of water–glycerol solution (mm^2/s)
Ω	angular velocity of impeller (rpm)
ω	angular velocity of the washer (rpm)

experimentally [23]. The swirled air flow over the cell suspension, caused by air friction at the interface and the pressure difference between the periphery and center of the gas-air vortex, leads to a quasi-stationary flow with an axial counterflow in the suspension. Unlike conventional bioreactors, aerial vortex bioreactors perform gentle and efficient mixing of liquids, including viscous ones, without foaming or cavitation formation, hydraulic shocks, highly turbulent and stagnant zones, or local high-temperature zones. Vortex mixing also significantly improves mass transfer efficiency. As a result, gas-vortex bioreactors are at the forefront of bioreactor evolution for suspension cultivation of cells, tissues, and microorganisms and are continually expanding their applicability in modern technologies. Savelyeva et al. [24] have experimentally shown that when cultivating a recombinant *Escherichia coli* strain in an aerial bioreactor, the volume coefficient of oxygen transfer increases 3.6-fold, and the efficiency of expression of the target protein increases 2.2-fold.

The successful use of vortex mixing in cell cultures and tissues has caught the attention of researchers, prompting them to study the dynamics of vortex processes in cell suspensions. This requires an understanding of how vortex motion is formed during the interaction of different liquid and gaseous media, such as a gas vortex in an aqueous medium [25] or immiscible liquid media with different densities and viscosities [26]. Studies on the effects of two-phase and two-fluid vortex flows are best conducted in a closed vertical cylindrical container due to the limited number of determining parameters. In these vortex devices [27–29], each medium has a separate meridional circulation [30]. Unlike solid-state rotation, where the angular velocity is constant and the maximum linear velocity occurs at the periphery, rotating liquid medium does not follow this pattern. A significant difference is that the radial velocity at the interface between two immiscible media is non-zero, as the spinning medium spirally converges to the cylinder axis [31].

The most common phenomenon observed in the closed vortex motion is bubble vortex breakdown (VB), which is characterized by an abrupt deceleration along the axis of the vortex. This can lead to the formation of a zone of reverse flow or a recirculation zone that negatively impacts the cultivation of bio cultures due to poor mass transfer [3]. However, VB effects in bioreactor configurations have not been extensively studied. Yu et al. [32] investigate this phenomenon and its effect on the environment inside an open cylinder, with potential application as a tissue-engineering bioreactor [32]. They found that the oxygen concentration at the attached breakdown vortex center was significantly higher than at the main recirculation center, but the hydrodynamic stress levels were similar in both regions. Similar study [33] revealed that a Reynolds number range of $600 < Re < 1100$ could provide an optimal regime for tissue culture in similar vessels. This is based on the need to maximize mass transport and mixing while minimizing fluid-induced forces. Regardless of the type of bioreactor used [32–34], one can conclude that flow hydrodynamics of the culture medium is the key parameter determining mass transfer efficiency. Despite numerous computational and experimental studies, creating universal and highly efficient bioreactors is still challenging due to hydrodynamic restrictions. Therefore, close attention should be paid to the dynamics of fluid motion in bioreactors.

There is a lack of research on the swirling fluid flow in an aerial vortex bioreactor [35]. In an experimental study of swirling flows in a gas-vortex reactor, it was discovered that a strongly swirling jet forms at the reactor axis, similar to the case of two rotating liquids. The entire flow takes on the structure of a miniature gas-liquid tornado, and the radial velocity component slips at the interface. Despite the difference in density by over three orders of magnitude, the spiral air flow converging to the reactor axis creates a divergent vortex motion of the liquid medium [35,36].

Although significant advances have been made in the development of aerial vortex bioreactors, research in this area is still ongoing. The flow hydrodynamics of the culture medium is critical to the development of bioreactors, and therefore, studying the flow structure remains important and relevant. To fully understand the laws and phenomena of flow hydrodynamics in a vortex bioreactor, it is necessary to measure fluid flow rates not only in model fluids but also in cell cultures, tissues, and various classes of microorganisms.

The biological features of cultivated objects present significant difficulties for flow diagnostics. As a result of the vital activity of cells, exometabolites accumulate in the culture medium and alter the physical properties (density and viscosity) of the cell suspension over time, thereby changing flow regimes. For example, *Porphyridium* red microalgae synthesize polysaccharides in large quantities in intensive culture [37], while *Azotobacter* bacteria create alginic acids that form high-viscosity aqueous solutions [38].

The aim of this work is to identify the patterns of the vortex flow of the working fluid in an aerial vortex bioreactor equipped with a free-floating washer at the interface at various parameters of the activator spin. By knowing the spin parameters, one can determine the flow mode in any opaque culture medium. The data obtained in the work have both great fundamental and practical meaning for the further development of bio-vortex technologies.

2. Experimental setup and experimental methodology

The experimental study of the vortex flow was carried out in 8.5 L universal aerial vortex bioreactor (Fig. 1a, 1b). This bioreactor was characterized by a high oxygen mass transfer rate K_La of 6–8 h^{-1} and low energy consumption of 0.3 W/L [24]. The vortex gas flow was generated by an impeller (activator) (Fig. 1c) over the surface of the liquid with an angular velocity Ω of up to 1500 rpm. The side wall of the bioreactor was made of optically transparent glass. The radius (R) of the bioreactor vessel was 95 mm, and its height (H) was 300 mm.

Distilled water (density $\rho_w = 999$ kg/m^3; kinematic viscosity $\nu_w = 1$ mm^2/s) and a water–glycerol solution (volume fraction of glycerol of 65%; $\rho_g = 1150$ kg/m^3; $\nu_g = 15$ mm^2/s) were used as working liquids that overlapped the main classes of cell cultures, tissues and microorganisms in terms of density and kinematic viscosity parameters. Here and further, the subscript “w” denotes distilled water, and the subscript “g” refers to the aqueous glycerol solution. The main experimental studies were carried out when the reactor vessel was filled with 50% working fluid, at which the height of the working fluid $h = 150$ mm and $h/R = 1.58$, respectively. For comparison, Dusting et al. [3] used $H/R =$

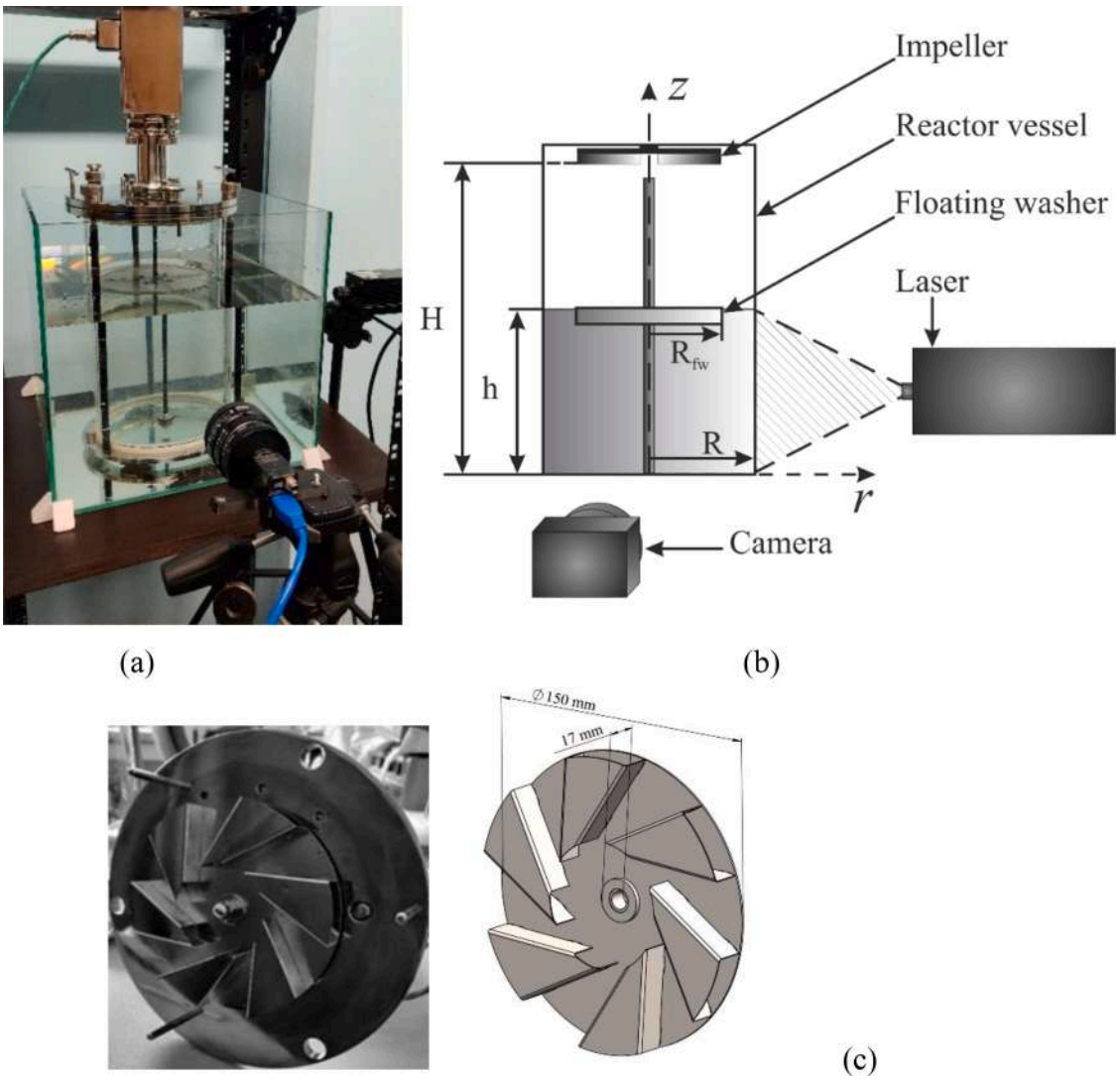

Fig. 1. A photo (a) and a diagram (b) of the experimental setup; a photo (left) and a diagram (right) of the impeller – activator (c).

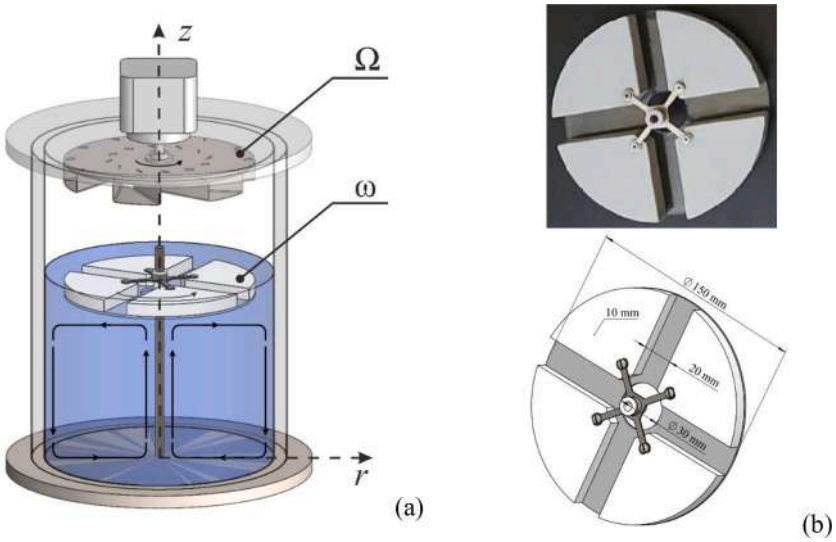

Fig. 2. The scheme of the aerial vortex bioreactor in the configuration with a floating washer (a), top view (up) and scheme (down) of a planar washer (b).

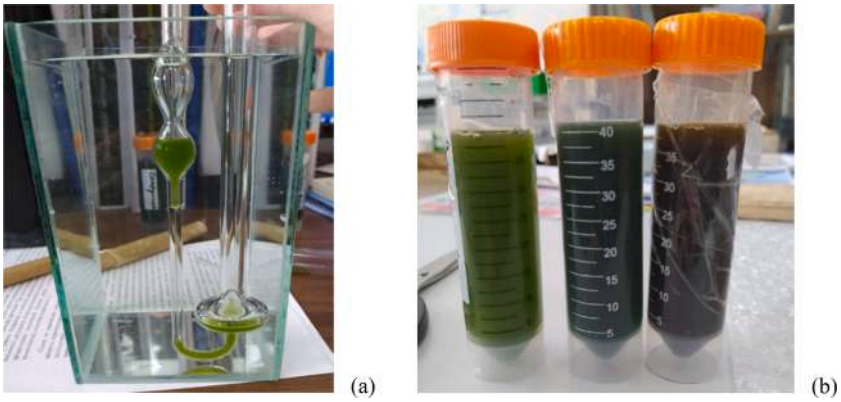

Fig. 3. Capillary viscometer with microalgae solution, b) microalgae samples.

1.5 and Sucosky et al. [1] used H/R = 1.17. Additional studies were performed for a smaller filling of the reactor vessel: h/R = 0.63 and 0.2.

During the experimental work, the configuration of the aerial vortex bioreactor equipped with a washer floating freely on the surface of the working fluid (Fig. 2a) was investigated. The radius of the washer R_{fw} was 75 mm, and its height h_{fw} was 12 mm. A gas vortex swirled the working fluid with a floating washer (Fig. 2b). A rod on the axis was used to center the washer. The presence of a fixed rod on the axis of the cylindrical container does not affect the fluid flow structure in the bioreactor [39]. The washer could freely rotate around the central rod and served as a reducer to decrease the angular velocity of the impeller Ω down to the angular velocity of the washer ω with the Ω/ω ratio being ~ 100. The washer stabilized the liquid motion and prevented the interface deformation.

The washer was designed to ensure additional gas exchange between the aerating gas vortex and the working fluid. The washer had four radial channels and a central hole. The washer was immersed in the liquid in such a way that some liquid was above the surface of the washer in radial channels and contacted air. Upon rotation of the liquid in the bioreactor equipped with a free-floating washer, the liquid in the channels and under the washer per se, being affected by the centrifugal force, moved to the periphery due to viscous friction. In the axial area above the washer, there was a minimum pressure due to which the liquid was sucked into the central orifice of the washer and appeared above it in radial channels through which it spread to the periphery of the cylinder to form a meridional liquid motion. Therefore, the presence of a floating washer did not impede the gas exchange between the swirled air and the working fluid.

Particle image velocimetry (PIV) was used to observe the vortex motion of the working liquid in the bioreactor. PIV provides instantaneous velocity distribution in the investigated cross-section and a flow pattern within the two-dimensional plane of a light sheet. The light sheet was formed by a laser of the PIV measurement system, and the image was recorded by the camera through the optically transparent side wall of the bioreactor (Fig. 1b). Measurements were performed in the vertical cross-section passing through the reactor axis, and in a horizontal cross-section under a floating washer and near the bottom at a distance of 2 mm. For reducing optical aberrations and thermostabilizing, the aerial vortex bioreactor was placed into a glass container sized 300 × 300 × 400 mm filled with tap water.

The PIV system consisted of a double-pulsed Nd:YAG Beamtech Vlite-200 laser (wavelength, 532 nm; repetition rate, 15 Hz; pulse duration, 10 ns; pulse energy, 200 mJ), an IMPERX IGV-B2020 CCD camera (8 bits per pixel; matrix resolution 2056 × 2060 pixels, with a 1.3″ optical format equipped with a Nikon SIGMA 50 mm f/2.8D lens), and a synchronizing processor. The two-dimensional velocity fields were calculated using the commercial ActualFlow software, Version 1.18.8.0. The thickness of the laser light sheet formed by a cylindrical lens to illuminate tracer particles was ~ 0.8 mm in the measurement plane. Polyamide beads (density, 1030 kg/m^3; diameter, ~ 10 μm) were employed as seeding light-scattering particles for PIV measurements [36,40].

For every set of experimental conditions, 300 images were accumulated and averaged to increase the signal-to-noise ratio. Uncertainty of PIV measurements was not above 5%. Time delay between the two images was varied from 100 to 800 ms depending on fluid type and rotation rate. The particle concentration has been selected in a way that ensured average values of 5–10 particles for a computational region of 32×32 pixels. The size of the particles in the image ranged from 1.5 to 2.5 pixels, and the maximum measured particle displacement within the computational domain was 8 pixels or less. The velocity fields were calculated using the iterative cross-correlation algorithm with a continuous window shift and deformation and 75% overlap of the interrogation windows in order to have a relatively large dynamic range (the span between the maximal and minimal velocity values). The spatial resolution was 70 vectors per 180 mm (or one vector per 2.57 mm)

3. A vortex structure formation at different degrees of bioreactor filling with a working medium

Viscosity measurements in microalgae suspension of various systematic groups were performed using a VPJ-4 capillary viscometer placed in a transparent vessel with water for better thermoregulation and thermal stabilization (Fig. 3a). To obtain a more accurate result, the experiment was carried out three times for each sample at 23.5 °C. Fig. 3 shows photographs of the measurement process and algae samples. Green marine microalgae *Tetraselmis viridis* Rouch., marine diatoms *Phaeodactylum tricornutum* Bohlin, marine red microalgae *Porphyridium purpureum* (Bory) Drew et Ross, archaea from hypersalted Lake Sasyk and freshwater cyanobacteria *Arthrospira platensis* (Nordstedt) *Gomont* were studied in the work.

The final value of the measured kinematic viscosity was obtained by averaging over all values and was 1.11 mm^2/s for green algae in Black Sea water, 1.21 mm^2/s for cyanobacteria in fresh water, 1.16 mm^2/s for diatoms in Black Sea water, 3.62 mm^2/s for red algae in Black Sea water, and 2.82 mm^2/s for archaea in hypersalted water.

The resulting kinematic viscosity values of almost all the solutions considered were close to the viscosity of water. The exception was archaea in hyper salted water, whose kinematic viscosity was almost three times higher than the viscosity of water. On the other hand, semi-liquid gelatin or agarized nutrient media, which have a viscosity of 4–12 mm^2/s, were used for growing microbial cultures. In addition, both the density and kinematic viscosity of the cultivated media could significantly increase during the cultivation process per se. As an additional example, we can present data on intensive cultivation in a gas-vortex

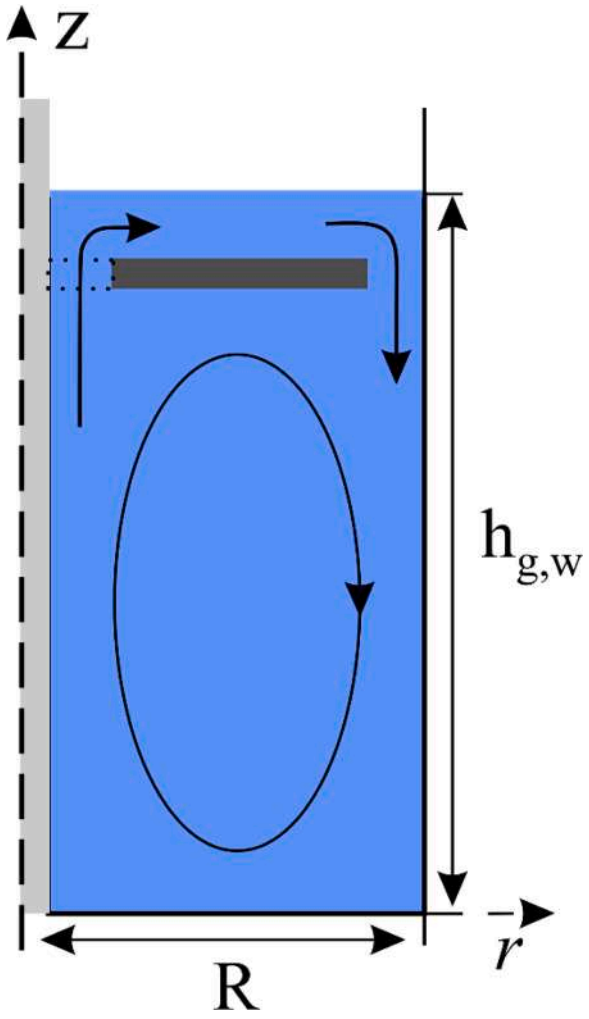

Fig. 4. Device and flow schematics in an aerial bioreactor equipped with a washer.

bioreactor of red *Porphyridium purpureum* microalgae with a change in the viscosity of the medium during cultivation from 1.16 mm^2/s (first day) to 15.07 mm^2/s (18th day of cultivation).

The studies carried out in this work using two media with a viscosity of 1 and 15 mm^2/s allow one to obtain the characteristic boundary flow regimes for the main operating modes of an aerial vortex bioreactor.

Flows within cylinders with a rotated disk on the surface or free washer are typically classified within the fluid dynamics literature in terms of their Reynolds number [41], $Re = V_{ang}R/\nu = (\omega R_{fw})R/\nu$, and the vessel aspect ratio h/R, where V_{ang} is the linear velocity of the washer rotation at its radius R_{fw}; ω and R_{fw} present the angular velocity of the washer and its radius; ν is the kinematic viscosity; R is the radius of the working section; and *h* is the fluid depth. *Re* represents the degree to which inertial forces dominate over viscous forces. The use of such dimensionless parameters means that the flow measurements can be scaled with changes in vessel properties. Scalability, which seems to have been overlooked during previous, more specialized, bioreactor design processes, is important in the context of the growing need to produce bioreactors capable of larger yields.

When the washer is rotating at a constant velocity, angular momentum is imparted to the fluid within the cylinder, causing a flow that is predominately azimuthal. The resulting flow in the radial and axial directions is relatively weak compared to the azimuthal flow; however, it constitutes the key mechanism for both fluid mixing and internal shearing, and, therefore, is of great interest to this study.

Fig. 4 shows the flow schematic of meridional motion in the model fluid at constant ω. Since the problem is axisymmetric, Fig. 4 shows half of the field in the liquid, where the left edge of the image corresponds to the axis of the reactor vessel, and the right edge corresponds to the periphery. On the axis of the cylinder, there is a fixed rod, depicted by a gray vertical rectangle.

A dark horizontal rectangle schematically indicates a washer with a central hole. The blue color represents liquid. The black arrows indicate the direction of the fluid flow. In this case, the flow topology is the simplest: the entire fluid undergoes the centrifugal circulation. Some liquid ascending near the central rod goes through the gap between the

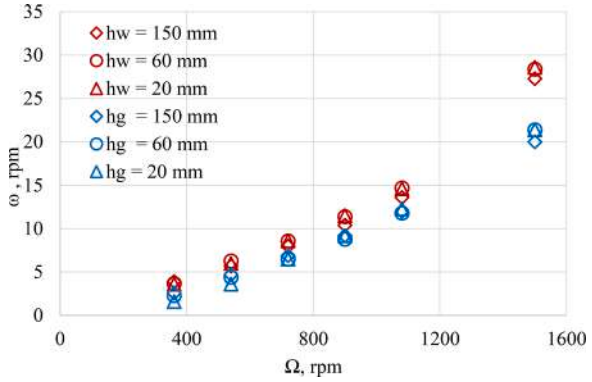

Fig. 5. Dependence of the rotation velocity of the flat washer on the rotation velocity of the activator for water (red) and water–glycerol solution (blue).

Table 1
Dependence of the rotation frequency of the planar washer on the rotation of the activator.

Water	h_w = 150 mm			h_w = 60 mm			h_w = 20 mm		
Ω, rpm	ω, rpm	V_{ang}, mm/s	*Re*	ω, rpm	V_{ang}, mm/s	*Re*	ω, rpm	V_{ang}, mm/s	*Re*
360	3.9	30.8	2923.3	3.7	29.3	2781.6	3.6	27.9	2647.4
540	5.7	44.4	4220.9	6.3	49.5	4705.7	6	47.1	4474.5
720	8	62.8	5966	8.6	67.4	6406	8.6	67.4	6398.5
900	10.4	81.2	7718.5	11.4	89.1	8464.3	11.5	90.4	8591
1080	13.6	107.1	10,172	14.7	115.4	10,962.5	14.6	114.9	10,917.8
1500	27.3	214.1	20,336.6	28.4	223.2	21,248.6	28.6	224.2	21,298.6
Water–glycerol solution	h_g = 150 mm			h_g = 60 mm			h_g = 20 mm		
Ω, rpm	ω, rpm	V_{ang}, mm/s	*Re*	ω, rpm	V_{ang}, mm/s	*Re*	ω, rpm	V_{ang}, mm/s	*Re*
360	2.6	20.3	128.3	2.3	18.4	116.3	1.6	12.2	77.1
540	4.7	36.8	233.2	4.4	34.6	219.3	3.6	28.3	179.5
720	6.9	54.1	342.5	6.5	51.2	324.2	6.5	50.6	320.7
900	9.2	72.5	458.9	8.8	69.2	438.5	9.2	72.5	458.9
1080	12	94.2	596.6	11.8	92.4	585.2	12.3	96.2	609
1500	20	157	994.3	21.4	168.2	1065.4	21.4	168.2	1065.4

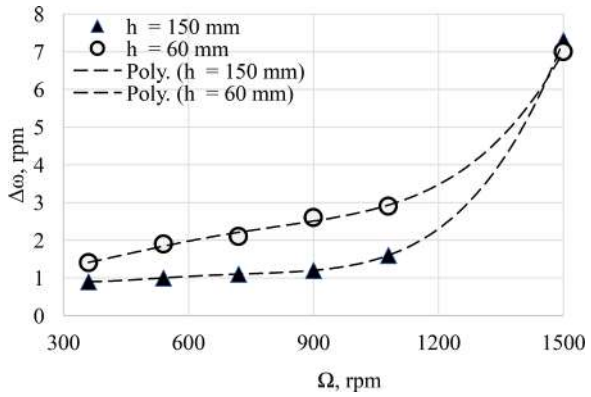

Fig. 6. The difference in the rotation velocity of the flat washer $\Delta\omega = \omega_w - \omega_g$ as a function of the rotation velocity of the activator when using the fluid of different viscosity for two fills $h = 60$ (circle) and 150 mm (triangle).

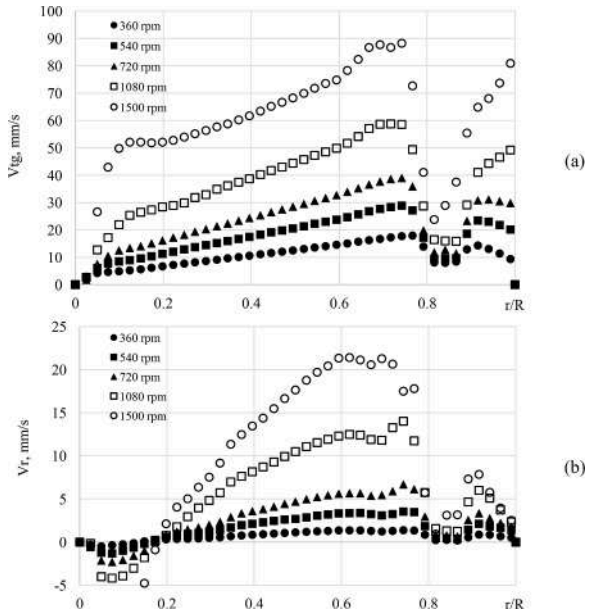

Fig. 7. The profiles of the azimuthal (a) and radial (b) velocity components in the fluid at a distance of 2 mm from the floating washer at different Ω for h_g = 150 mm.

rod, $r = 3$ mm, and the washer, $r_{wi} = 15$ mm, reaches the free surface, $z = h_{g,w} = 150$ mm, turns outwards and goes above the washer up to the side wall, $R = 95$ mm, turns downwards passing the gap between the washer and the side wall and descends along the side wall. The remaining liquid circulates below the washer in the region enclosed by the black curve in Fig. 4. The flow topology changes as ω varies.

The experiment served to determine the dependence between the rotation frequency of the flat washer on the rotation frequency of the activator at different volumes of bioreactor filling by 50, 20 and 10% for water and an aqueous glycerol solution; the data are presented in Table 1.

Fig. 5 shows the dependence of the rotation velocity of the flat washer on the rotation velocity of the activator for various fillings of the bioreactor. As it can be seen in Fig. 5, the rotation frequencies of a free-floating washer do not depend on the level of filling of the reactor tank with the working fluid, but there is some difference associated with the kinematic viscosity of the working medium per se.

Fig. 6 shows the dependences $\Delta\omega(\nu) = \omega_w - \omega_g$ for $h = 60$ and 150 mm. One can see that as liquid viscosity rises, the rotation frequency of the washer ω(ν) decreases non-linearly with an increase in the rotation

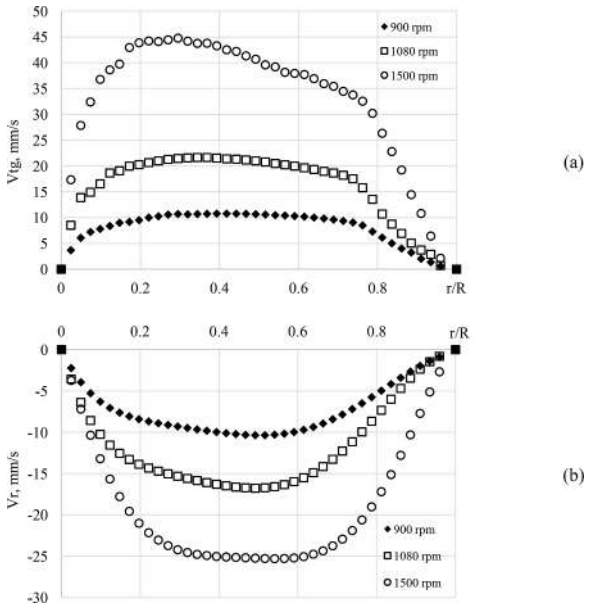

Fig. 8. The profiles of the azimuthal (a) and radial (b) velocity components in a liquid at a distance of 2 mm from the bottom at different Ω for h_g= 150 mm.

velocity of the activator, taking a significant difference $\Delta\omega = 7$ at the maximum rotation frequencies of the activator, regardless of the size of the working fluid layer. Therefore, based on the values of rotation frequency of a free-floating washer at Ω>1000, one can indirectly estimate both the viscosity of the medium, which changes directly during cultivation, and the hydrodynamic structure of the vortex motion in the bioreactor.

4. Experimental results and discussion: the flow structure in an aerial bioreactor

An experimental study of the flow structure in an aerial vortex bioreactor with a floating washer at the interface was carried out at various Ω in the range from 360 to 1500 rpm with 50% filling of the reactor with the working fluid. At $h_g = 150$ mm, the distance between the bottom of the reactor and the floating washer was 140 mm. At Ω values exceeding 1500 rpm, fluctuations in the interface of the liquid medium are observed; they can lead to destruction of cultured cells and tissues. The velocity fields and profiles of azimuthal (V_{tg}) and radial (V_r) velocity components in the liquid under the washer and near the stationary bottom of the bioreactor were obtained and analyzed using the PIV method. Fig. 7 shows the profiles of the tangential and radial velocity components at $\Omega \leq 1500$ measured at a distance of 2 mm under the rotating washer.

The profiles of the tangential velocity component are close to those of solid-rotation (Fig. 7a), and the positive profiles of the radial velocity component (Fig. 7b) indicate fluid motion diverging from the axis to the periphery. This type of the flow indicates that the circulating motion of the working fluid occurs under the washer. The dips in the velocity profiles at $r/R > 0.78$ are due to the fact that the radius of the floating washer is smaller than that of the reactor vessel. A slight increase in the velocity values at the periphery is caused by jet streams of liquid coming out of the radial channels of the washer through which the working fluid passing through the axial hole moves. Fig. 8 shows the profiles of the tangential and radial velocity components in a liquid at a distance of 2 mm from the bottom at different Ω for $h_g = 150$ mm. The maximum values of the tangential velocity component are halved due to the friction of the working fluid against the walls of the bioreactor cylinder. Meanwhile, near the bottom, the profiles of the radial velocity component change sign, characterizing the working fluid motion converging to

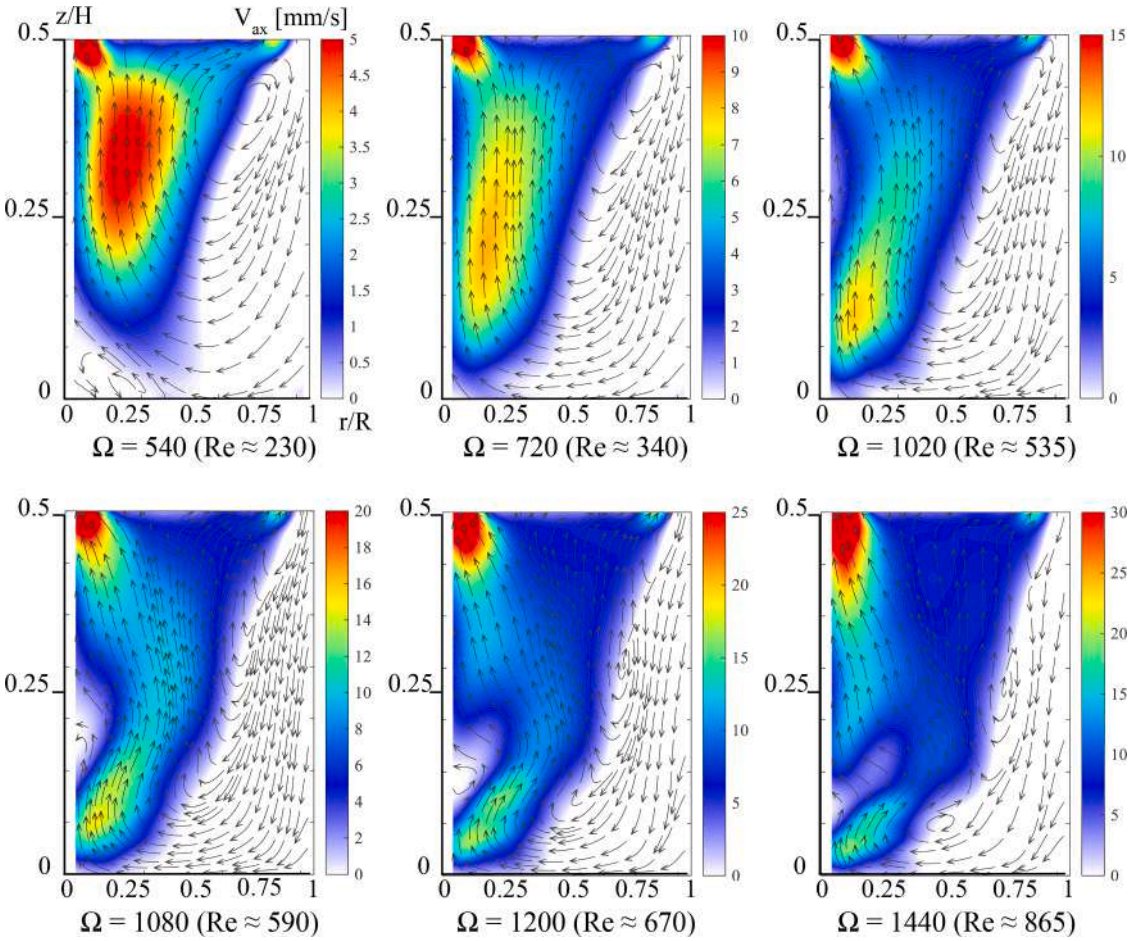

Fig. 9. Distribution of the axial velocity in the vertical section of the bioreactor and the evolution of vortex breakdown at increasing Ω for h_g = 150 mm.

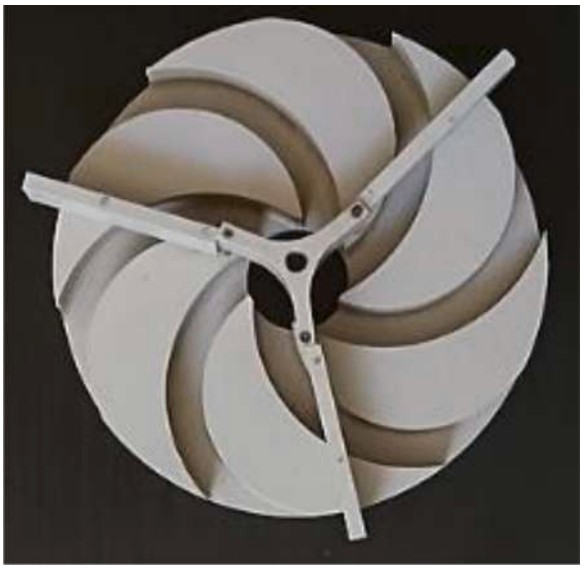

Fig. 10. Top view of sail washer.

the axis. Therefore, the presented results confirm the meridional motion of the working fluid in the vertical section of the bioreactor at all values of the activator rotation.

The measured velocity in the vertical section using the PIV method also confirms the presence of meridional circulation in the liquid. Fig. 9 shows the velocity vector fields in a liquid (water–glycerol mixture) under the washer and the scalar field of the axial velocity component, when the reactor was filled with a water–glycerol mixture by 50%. The scale to the right of the images refers to the value of the axial velocity component (V_{ax}) in mm/s. Here and below, the positive value of the axial velocity component is highlighted in color, and the area of negative velocity values in the direction from the floating washer to the bottom of the reactor is highlighted in white. Since there is a fixed rod on the cylinder axis, Fig. 9 shows half of the velocity fields in the liquid, where the left edge of the image corresponds to the axis of the reactor vessel, and the right edge corresponds to the periphery. The images show the circulating motion of the liquid under the floating washer. At Ω = 720 rpm, the circulation cell in the liquid is shown to occupy the entire volume, unlike the configuration with a free surface of the liquid, where the circulation cell reaches the bottom at large Ω. A strong flow in the axial area under the washer indicates that liquid is sucked into the central orifice of the washer.

Fig. 9 shows the evolution of the formation and development of the zone of reverse motion — the vortex breakdown with increasing Ω — on the axis. The given velocity fields demonstrate the appearance and disappearance of a bubble-like vortex breakdown in the axial region with increasing Ω (Fig. 9). Therefore, one can argue that the vortex structure in an aerial vortex bioreactor develops in a way similar to the case of a swirling flow in a cylindrical container with a rotating end and with no washer [41]. Accordingly, since the structures are the same, the similarity criterion such as the Reynolds number can be used to determine the flow regime. Since the vortex breakdown in the bioreactor takes place in the range of Ω from 1050 to 1440, the Reynolds number at which the vortex breakdown occurs lies in the range from 560 to 865.

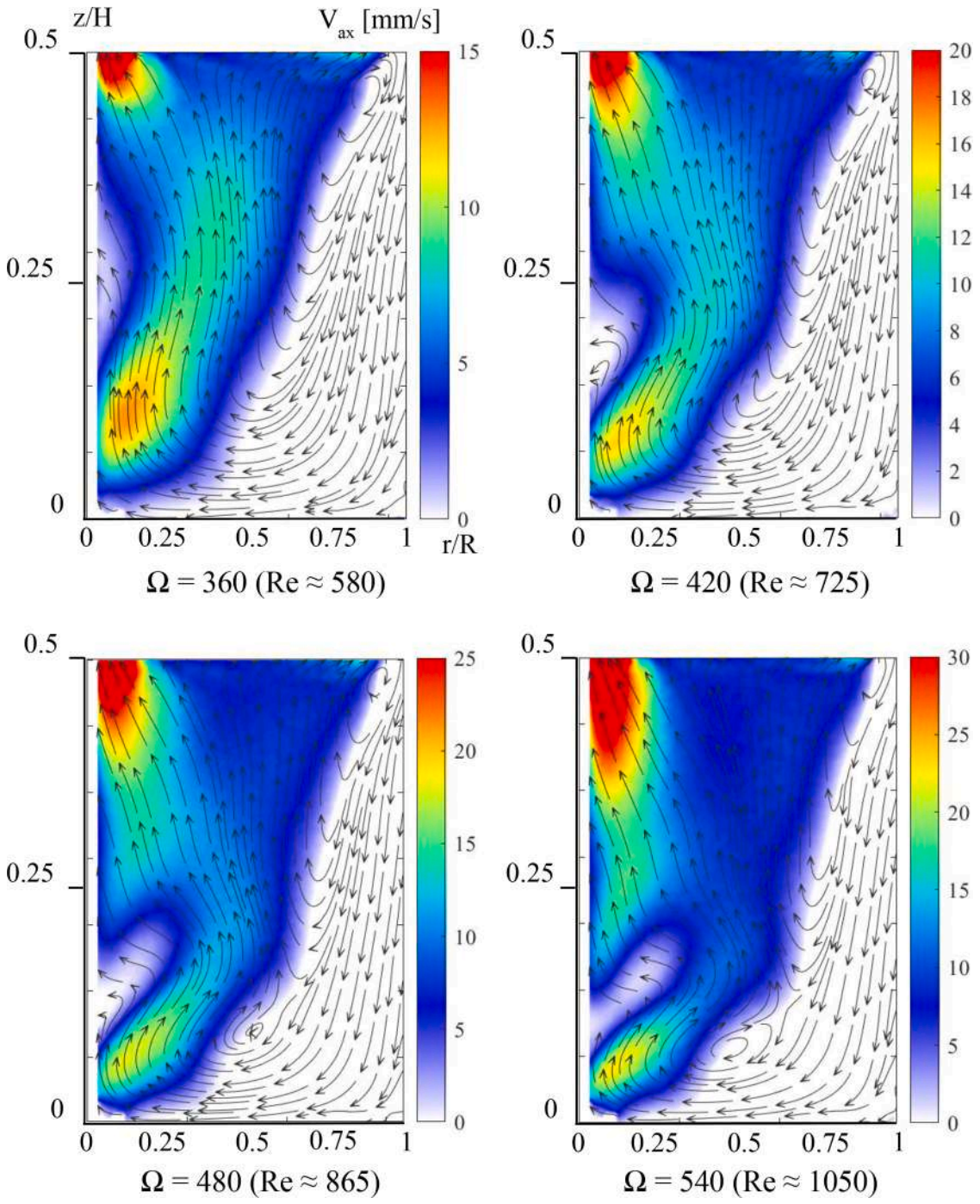

Fig. 11. Evolution of vortex breakdown for sailing washer at an increase of Ω for h_g = 150 mm.

Table 2
Comparison of the rotation frequency of the planar and sailing washers.

Forcing Ω, rpm	Planar washer ω, rpm	V_{ang}, mm/s	*Re*	Forcing Ω, rpm	Sailing washer ω, rpm	V_{ang}, mm/s	*Re*
720	6.8	53.6	339.2	360	11.7	93.5	578.4
900	9.1	71.4	452.2	390	13.1	104.1	659.2
1020	10.7	84.2	533.3	420	14.4	114.4	724.5
1080	11.9	93.4	591.1	450	15.7	125.2	793.0
1140	12.5	98.3	622.4	480	17.2	136.6	864.8
1200	13.4	105.6	668.6	510	18.7	148.4	939.8
1440	17.4	136.6	864.9	540	20.9	166.1	1051.6

The vortex breakdown observed by Escudier [41] at the aspect ratio $H = h_g/R = 150/95 = 1.57$ occurs in the range *Re* from 1100 to 1900. Thus, the development of vortex breakdown in the bioreactor occurs at significantly lower Reynolds numbers than in the Escudier work. It is due to the fact that the washer radius is smaller than that of the reactor vessel. The ratio between the reactor radius and the washer radius is approximately 1.27, and Yu et al. [42] have shown that with this ratio, the vortex breakdown region is shifted to smaller *Re*. An increase in the flow velocity at the periphery caused by jet streams of liquid coming out of the radial channels of the washer affects the structure. In this case, a more intense upward flow is formed, since both surfaces of the disk work, providing a greater pressure gradient due to the forces of viscous friction.

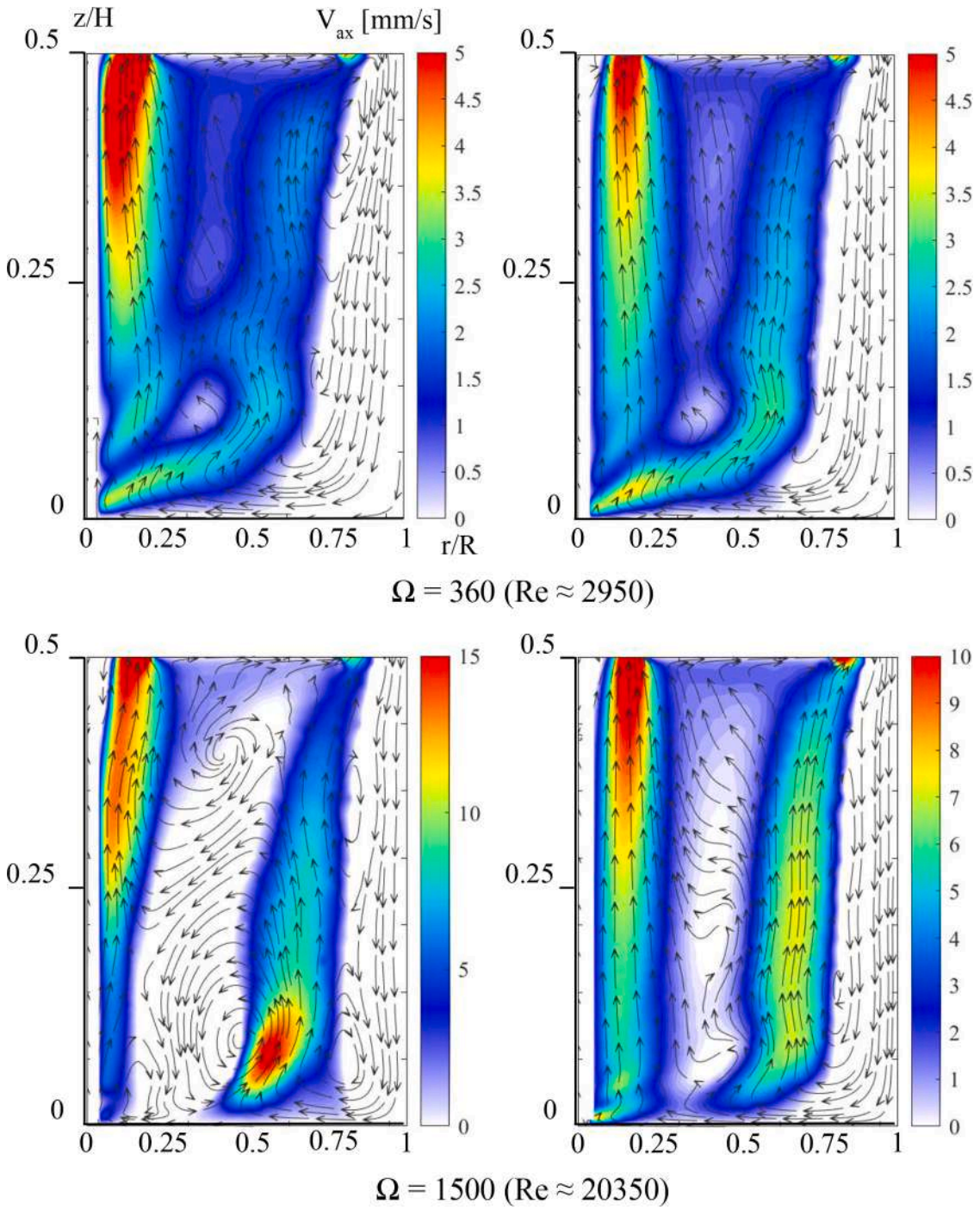

Fig. 12. Examples of the velocity distribution in the vertical section of the bioreactor: (left) the instantaneous velocity; (right) the average velocity field for the extreme Ω values at $h_w = 150$ mm.

In other words, the Reynolds number *Re*, at which a bubble-like vortex breakdown occurs in the bioreactor, differs from the Reynolds number for a cylindrical container with a rotating end [41]. Since the flow structures are similar in both cases, it is possible to select the coefficient α, depending on the system parameters, at which the new Reynolds number Re_{bio} for a liquid in an aerial vortex bioreactor will be the same as in the case of a cylindrical container with a rotating end. To properly determine α, one needs to take into account the kinematic viscosity ν of the liquid, since the culture medium and the rotation frequency of the washer ω may change during cell growth, since when the viscosity of the liquid changes, and the friction force acting on the washer will change as well. Taking into account all these observations, Re_{bio} can be presented as:

$$Re_{bio} = \alpha(\omega, \nu)Re = \alpha(\omega, \nu)wR_{fw}R / \nu$$

At a viscosity $\nu = 15$ mm^2/s, the variable coefficient α depending on the system parameters is the estimated value $\alpha(\omega, \nu) \approx 2$ for the Reynolds number, at which it will be possible to compare *Re* for a closed cylindrical container with Re_{bio} for a liquid in a vortex bioreactor.

Obviously, the transfer characteristic for *Re*, in addition to Ω, is also determined by ω, which depends on the washer design. For example, the effect of the vortex airflow will be much stronger on the washer with sails (Fig. 10).

Fig. 11 shows the distributions of velocity fields for the design of a

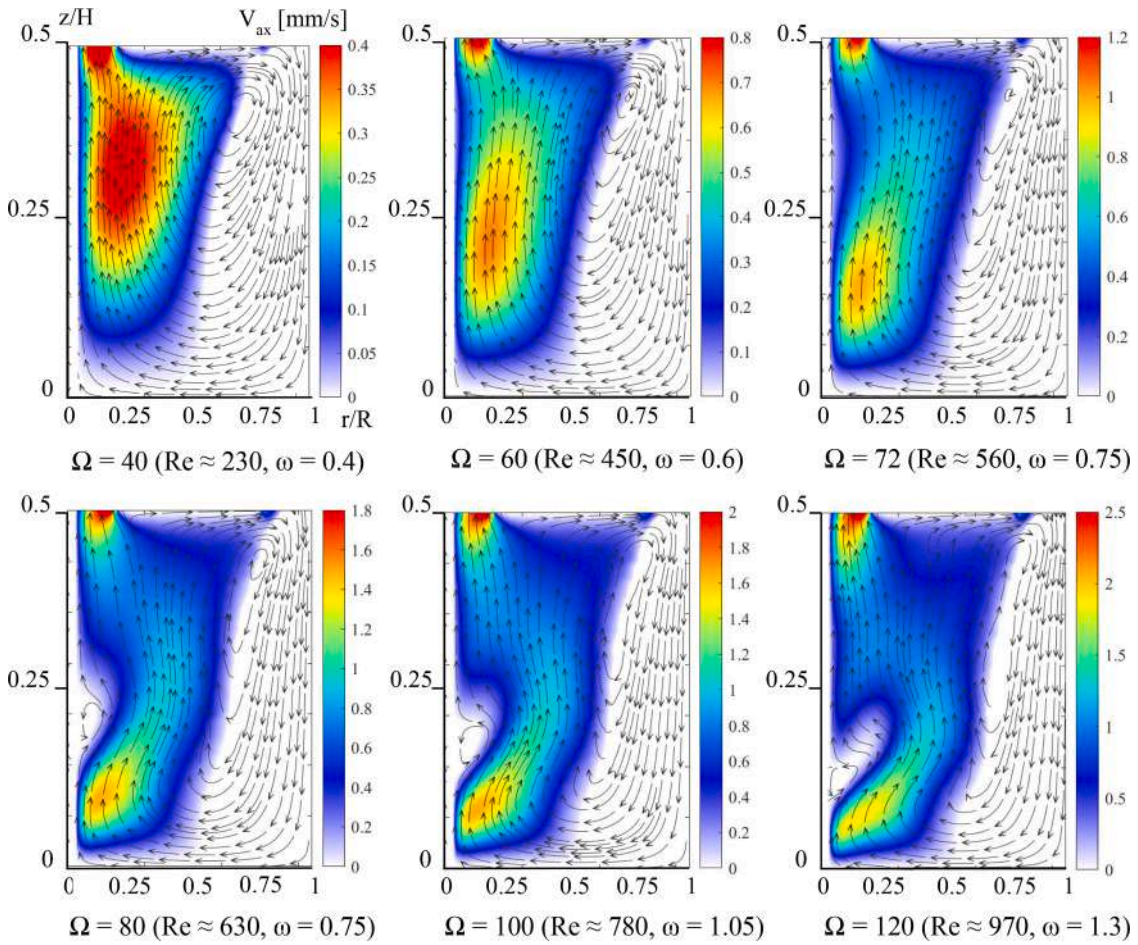

Fig. 13. Velocity distribution in the vertical section of the bioreactor and the evolution of vortex breakdown at low Ω values for water (h_w = 150 mm).

free-floating washer with sails as the activator velocity increases, illustrating the presence of a return flow zone on the reactor axis.

Table 2 shows the prescribed driver frequency Ω, the resulting washer frequency ω, the maximal washer velocity $V_{ang} = \omega R_{fw}$, and the Reynolds number $Re = V_{ang}R/\nu_g$. In this case, according to Table 2, the angular velocity of rotation of the sail washer significantly exceeds that of the original washer submerged in the working fluid. The occurrence and evolution of the return flow region in the vicinity of the reactor axis — the bubble-like breakdown of the vortex — are observed in the range of Ω from 360 to 540 for case of the sail washer. The characteristics of the vortex structure registered in the flow, based on the Reynolds number calculated from the angular velocity of washer rotation, represent a similar dynamic of formation of the return flow region in the axial zone, but at much lower velocities of activator rotation. Therefore, the Reynolds number remains a parameter characterizing the hydrodynamic similarity.

Let us consider another specific case: using the distilled water with a kinematic viscosity $\nu_w = 1$ mm^2/s as a model liquid. Fig. 12 shows the instantaneous velocity fields and those averaged over 300 instantaneous velocity fields measured by PIV in a configuration with a flat washer for rotation velocities Ω that overlap operating modes. The instantaneous values illustrate the formation of a complex turbulent flow structure with a predominant meridional circulation motion, which can be clearly observed in the averaged velocity fields. Therefore, one can argue that at low values of the kinematic viscosity of the working fluid (distilled water), the velocity values on the reactor axis do not undergo any changes: there is a strong upward flow along the reactor axis (Fig. 12) over the entire range of rotation frequencies of the activator.

Since the kinematic viscosities of the glycerol mixture and water differ approximately 15-fold, then, using the Reynolds number to determine the hydrodynamic similarity, one can assume that by reducing the rotation frequency of the activator on the reactor axis 15-fold, it is possible to obtain a return flow area for the case of using distilled water as a working fluid. Fig. 13 shows the modes and results of forming a return flow area for water. At that, the area of reverse motion on the reactor axis for this medium, which has a low kinematic viscosity, is observed with a significant decrease in rotation velocity of the activator (approximately 12–14 times) with respect to the viscous water–glycerol mixture and, accordingly, a reduced angular velocity of the washer rotation. In this case, the absolute velocity values decrease in proportion to the angular velocity of the activator and the rotation velocity of the floating washer, respectively.

Minor deviations of the activator setting parameter can be explained by the nonlinear transfer coefficient between activator rotation and rotation of the floating washer. Meanwhile, the Reynolds number determining the hydrodynamic similarity remains unchanged (Fig. 9 and 13).

It can be inferred that even with small kinematic viscosities of the working medium, close to the values of water, the Reynolds number can be used to describe flow regimes in a bioreactor. However, it should be taken into account that the viscosity of the cultivated medium may rise as concentration of cells and tissues increases, which will change the flow hydrodynamics in the reactor per se. For example, a fivefold change in viscosity with respect to the initial value may lead to formation of stagnant recirculation zones in the axial region of the reactor operating in the 500–1000 rpm rotation frequency range, in which cells with a large specific cavity will be deposited, despite the fact that the ambient velocity will be high.

5. Conclusions

A detailed study of the flow structure in an aerial vortex bioreactor having a configuration with a floating washer at various parameters of the flow swirl has been carried out. The patterns of the vortex motion of the model medium have been determined depending on its volume, viscosity and activator rotation intensity. The air vortex generated by the impeller (activator) above the surface of the liquid spins the working fluid with a floating washer. When the activator is rotating, a centrifugal meridional circulation is shown to occur under the washer, and an ascending swirling jet is formed near the bioreactor axis. As the rotation velocity of the activator increases, there may be operating regimes in which a bubble-like vortex breakdown is formed on the reactor axis.

Despite the complex configuration of the flow stabilizing device (a free-floating washer), the observed vortex structure and its dynamics were found to coincide with the structure of a confined vortex flow in a cylindrical container with no washer for both single-fluid [41] and two-fluid systems [43], but the vortex breakdown develops at significantly lower Reynolds numbers. A more intense upward flow is assumingly formed due to the twofold difference in values, since both surfaces of the disk (the floating washer) work, thus providing a greater pressure gradient due to viscous friction forces as a result of the action of the centrifugal force. These results confirm the conclusion that the vortex breakdown is an indicator of the flow regime. By comparing these findings with the known data on vortex breakdown in a cylindrical container, it is possible to select an upgraded coefficient that will allow one to determine the flow regime for practical use of an aerial vortex bioreactor and analyze the flow structure based on the washer rotation. When cultivating opaque cell suspensions by the free-floating washer rotation, it is possible to uniquely determine the topology of fluid motion at a given activator rotation value.

The resulting data are of great interest for developing the methods to grow cell cultures in a bioreactor and identify the kinematic parameters of opaque media of the cultured biomaterial.

Data availability

Data will be made available on request.

CRediT authorship contribution statement

Igor V. Naumov: Conceptualization, Validation, Formal analysis, Resources, Writing – original draft, Supervision, Project administration, Funding acquisition. **Ruslan G. Gevorgiz:** Conceptualization, Validation, Resources, Writing – review & editing. **Sergey G. Skripkin:** Methodology, Formal analysis, Investigation, Data curation, Visualization. **Maria V. Tintulova:** Investigation, Visualization. **Mikhail A. Tsoy:** Investigation, Data curation, Visualization. **Bulat R. Sharifullin:** Methodology, Formal analysis, Investigation, Data curation, Visualization, Writing – original draft.

Declaration of Competing Interest

The authors declare that they have no known competing financial interests or personal relationships that could have appeared to influence the work reported in this paper.

Data availability

Data will be made available on request.

Acknowledgements

This research of flow transformations in a vortex bioreactor was funded by the Russian Science Foundation, grant number 19-19-00083, development of optical diagnostic technique was carried out within the framework of a state contract with IT SB RAS. The authors are grateful to the financial support for biomaterial study provided by the Institute of Biology of the Southern Seas of RAS (No 121030300149-0).

Supplementary materials

Supplementary material associated with this article can be found, in the online version, at doi:10.1016/j.cep.2023.109467.

References

[1] P. Sucosky, D.F. Osorio, J.B. Brown, G.P. Neitzel, Fluid mechanics of a spinner-flask bioreactor, Biotechnol. Bioeng. 85 (2004), https://doi.org/10.1002/bit.10788.
[2] P. Yu, T.S. Lee, Y. Zeng, H.T. Low, Fluid dynamics of a micro-bioreactor for tissue engineering, Fluid Dyn. Mater. Process. 1 (2005).
[3] J. Dusting, J. Sheridan, K. Hourigan, A fluid dynamics approach to bioreactor design for cell and tissue culture, Biotechnol. Bioeng. 94 (2006), https://doi.org/10.1002/bit.20960.
[4] K.V.K. Boodhoo, M.C. Flickinger, J.M. Woodley, E.A.C. Emanuelsson, Bioprocess intensification: a route to efficient and sustainable biocatalytic transformations for the future, Chem. Eng. Process. (2022) 172, https://doi.org/10.1016/j.cep.2022.108793.
[5] C. Kasper, M. Griensven, R. Pörtner, Bioreactor Systems for Tissue Engineering II, Springer, Berlin Heidelberg, Berlin, Heidelberg, 2010, https://doi.org/10.1007/978-3-642-16051-6.
[6] Z. Huang, Y. Shuai, C. Ren, Y. Yang, J. Sun, J. Wang, Y. Yang, Effects of internal structures on mass transfer performance of jet bubbling reactor, Chem. Eng. Process. 175 (2022), https://doi.org/10.1016/j.cep.2022.108936.
[7] D. Kumar, N. Gangwar, A.S. Rathore, M. Ramteke, Multi-objective optimization of monoclonal antibody production in bioreactor, Chem. Eng. Process. (2022) 180, https://doi.org/10.1016/j.cep.2021.108720.
[8] F. Ramonet, B. Haddadi, C. Jordan, M. Harasek, Modelling and design of optimal internal loop air-lift reactor configurations through computational fluid dynamics, Chem. Eng. Trans. (2022) 94, https://doi.org/10.3303/CET2294136.
[9] P. Jaibiba, S. Naga Vignesh, S. Hariharan, Working principle of typical bioreactors. Bioreactors, Elsevier, 2020, pp. 145–173, https://doi.org/10.1016/B978-0-12-821264-6.00010-3.
[10] R. Pohorecki, Fluid mechanical problems in biotechnology, Biotechnologia (2002) 60–77.
[11] F. Garcia-Ochoa, V.E. Santos, E. Gomez, Stirred Tank Bioreactors. Comprehensive Biotechnology, Elsevier, 2011, pp. 179–198, https://doi.org/10.1016/B978-0-08-088504-9.00108-2.
[12] X.T. Wang, Z.N. Wen, Y. Luo, B.C. Sun, Y.Y. Shao, G.W. Chu, Oxygen mass transfer intensification in an inner-loop rotor-stator reactor: production of sodium gluconate as an example, Chem. Eng. Process. (2021) 160, https://doi.org/10.1016/j.cep.2020.108290.
[13] H.W. Yen, I.C. Hu, C.Y. Chen, J.S. Chang, Design of photobioreactors for algal cultivation, Biofuels Algae (2013), https://doi.org/10.1016/B978-0-444-59558-4.00002-4.
[14] A.O. Kuzmin, Confined multiphase swirled flows in chemical engineering, Rev. Chem. Eng. 37 (2021) 31–68, https://doi.org/10.1515/revce-2019-0019.
[15] R.S. Cherry, E.T. Papoutsakis, Hydrodynamic effects on cells in agitated tissue culture reactors, Bioprocess Eng. 1 (1986), https://doi.org/10.1007/BF00369462.
[16] D.W. Murhammer, C.F. Goochee, Sparged animal cell bioreactors: mechanism of cell damage and pluronic F-68 protection, Biotechnol. Prog. 6 (1990), https://doi.org/10.1021/bp00005a012.
[17] Y. Chisti, Animal-cell damage in sparged bioreactors, Trends Biotechnol. 18 (2000), https://doi.org/10.1016/S0167-7799(00)01474-8.
[18] R.G. Gevorgiz, A.A. Gontcharov, S.N. Zheleznova, L.V. M.alakhova, T.E. Alyomova, T. Maoka, M.V. N.ekhoroshev, Biotechnological potential of a new strain of Cylindrotheca fusiformis producing fatty acids and fucoxanthin, Bioresour. Technol. Rep. 18 (2022), https://doi.org/10.1016/j.biteb.2022.101098.
[19] E.T. Papoutsakis, Fluid-mechanical damage of animal cells in bioreactors, Trends Biotechnol. 9 (1991), https://doi.org/10.1016/0167-7799(91)90145-8.
[20] W. Hu, C. Berdugo, J.J. Chalmers, The potential of hydrodynamic damage to animal cells of industrial relevance: current understanding, Cytotechnology 63 (2011), https://doi.org/10.1007/s10616-011-9368-3.
[21] L.N. Tsoglin, B.V. G.abel', T.N. Fal'kovich, V.E. Semenenko, Closed photobioreactors for microalgal cultivation, Russ. J. Plant Physiol. 43 (1996).
[22] E.O. Ojo, H. Auta, F. Baganz, G.J. Lye, Engineering characterisation of a shaken, single-use photobioreactor for early stage microalgae cultivation using Chlorella sorokiniana, Bioresour. Technol. 173 (2014), https://doi.org/10.1016/j.biortech.2014.09.060.
[23] Y.A. Ramazanov, V.I. Kislykh, I.P. Kosyuk, N.V. Bakuleva, V.V. Shchurikhina, Industrial production of vaccines using embryonic cells in gas-vortex gradient-less bioreactors, in: A.M. Egorov (Ed.), New Aspects of Biotechnology and Medicine, Nova Scientific Books, New York, 2007, pp. 87–91.
[24] A.V. Savelyeva, A.A. Nemudraya, V.F. Podgornyi, N.V. L.aburkina, Y. A. Ramazanov, A.P. Repkov, E.V. K.uligina, V.A. Richter, Analysis of the efficiency of recombinant Escherichia coli strain cultivation in a gas-vortex bioreactor, Biotechnol. Appl. Biochem. 64 (2017), https://doi.org/10.1002/bab.1527.

[25] A.V. Byalko, Underwater gas tornado, Phys. Scr. 88 (2013), https://doi.org/10.1088/0031-8949/2013/T155/014030.
[26] I.V. Naumov, B.R. Sharifullin, A.Y. Kravtsova, V.N. Shtern, Velocity jumps and the Moffatt eddy in two-fluid swirling flows, Exp. Therm. Fluid Sci. 116 (2020), https://doi.org/10.1016/j.expthermflusci.2020.110116.
[27] V. Shtern, Cellular Flows: Topological Metamorphoses in Fluid Mechanics, 2018, https://doi.org/10.1017/9781108290579.
[28] E.V. Stepanova, T.O. Chaplina, Yu.D. Chashechkin, Experimental investigation of oil transport in a compound vortex, J. Appl. Mech. Tech. Phys. 54 (2013) 408–414, https://doi.org/10.1134/S0021894413030097.
[29] V. Shtern, I. Naumov, Swirl-decay mechanism generating counterflows and cells in vortex motion, J. Eng. Thermophys. 30 (2021) 19–39, https://doi.org/10.1134/S1810232821010033.
[30] I.V. Naumov, M.A. Herrada, B.R. Sharifullin, V.N. Shtern, Slip at the interface of a two-fluid swirling flow, Phys. Fluids 30 (2018), 074101, https://doi.org/10.1063/1.5037222.
[31] I.V. Naumov, B.R. Sharifullin, S.G. Skripkin, M.A. Tsoy, V.N. Shtern, A Two-Story Tornado in a Lab, Springer Geology, 2022, https://doi.org/10.1007/978-3-030-85851-3_4.
[32] P. Yu, T.S. Lee, Y. Zeng, H.T. Low, Effect of vortex breakdown on mass transfer in a cell culture bioreactor, Mod. Phys. Lett. B (2005), https://doi.org/10.1142/S0217984905009869.
[33] S.J. Cogan, K. Ryan, G.J. Sheard, The effects of vortex breakdown bubbles on the mixing environment inside a base driven bioreactor, Appl. Math. Model. 35 (2011), https://doi.org/10.1016/j.apm.2010.09.039.
[34] M. Ramezani, B. Kong, X. Gao, M.G. Olsen, R.D. Vigil, Experimental measurement of oxygen mass transfer and bubble size distribution in an air-water multiphase Taylor-Couette vortex bioreactor, Chem. Eng. J. (2015) 279, https://doi.org/10.1016/j.cej.2015.05.007.
[35] B.R. Sharifullin, S.G. Skripkin, I.V. Naumov, Z. Zuo, B. Li, V.N. Shtern, Intense vortex motion in a two-phase bioreactor, Water 15 (2022) 94, https://doi.org/10.3390/w15010094.
[36] I.V. Naumov, R.G. Gevorgiz, S.G. Skripkin, B.R. Sharifullin, Experimental investigation of vortex structure formation in a gas-vortex bioreactor, Thermophys. Aeromech. 29 (2023), https://doi.org/10.1134/s0869864322050067.
[37] P. Fleck-Schneider, F. Lehr, C. Posten, Modelling of growth and product formation of Porphyridium purpureum, J. Biotechnol. 132 (2007), https://doi.org/10.1016/j.jbiotec.2007.05.030.
[38] G.A. Bonartseva, E.A. Akulina, V.L. Myshkina, V.V. V.oinova, T.K. Makhina, A. P. Bonartsev, Alginate biosynthesis by Azotobacter bacteria, Appl. Biochem. Microbiol. 53 (2017) 52–59, https://doi.org/10.1134/S0003683817010070.
[39] S. Sharma, P.B. Sachan, N. Kumar, R. Ranjan, S. Kumar, K. Poddar, Vortex breakdown control using varying near axis swirl, Phys. Fluids 33 (2021), https://doi.org/10.1063/5.0061025.
[40] I.V. Naumov, S.G. Skripkin, V.N. Shtern, Counterflow slip in a two-fluid whirlpool, Phys. Fluids 33 (2021), 061705, https://doi.org/10.1063/5.0055355.
[41] M.P. Escudier, Observations of the flow produced in a cylindrical container by a rotating endwall, Exp. Fluids 2 (1984) 189–196, https://doi.org/10.1007/BF00571864.
[42] P. Yu, T.S. Lee, Y. Zeng, H.T. Low, Characterization of flow behavior in an enclosed cylinder with a partially rotating end wall, Phys. Fluids 19 (2007), https://doi.org/10.1063/1.2731420.
[43] I.V. Naumov, B.R. Sharifullin, M.A. Tsoy, V.N. Shtern, Dual vortex breakdown in a two-fluid confined flow, Phys. Fluids 32 (2020), 061706, https://doi.org/10.1063/5.0012156.